JOURNAL OF CATALYSIS **158,** 439–451 (1996)
ARTICLE NO. 0045

Preparation of Pt/γ-Al_2O_3 Pellets with Internal Step-Distribution of Catalyst: Experiments and Theory

Panayiotis Papageorgiou, Douglas M. Price, Asterios Gavriilidis,[1] and Arvind Varma[2]

Department of Chemical Engineering, University of Notre Dame, Notre Dame, Indiana 46556

Received November 30, 1994; revised September 12, 1995

Step-type Pt/γ-Al_2O_3 catalyst pellets were prepared by coimpregnation and sequential impregnation of hexachloroplatinic and citric acids. A diffusion–adsorption model based on Fickian diffusion and Langmuir adsorption was formulated. The parameters of the model were determined from separate experiments. Adsorption constants were obtained in the absence of diffusional resistances, while effective diffusivities were obtained in the absence of adsorption or desorption. In order to extend the Langmuir adsorption equations to the multicomponent system, two new parameters were introduced, which accounted for solution effects and steric hinderances. Catalyst distribution inside the pellet and the effects of various impregnation parameters were predicted satisfactorily by the multicomponent diffusion–adsorption model. The platinum distribution of pellets prepared by the two impregnation techniques was similar, although sequential impregnation gave thinner catalyst step widths.

INTRODUCTION

Catalysts involving group VIII metals are usually prepared by dispersing the metal on a high-surface-area support, so that a large fraction of metal atoms becomes available for reaction. The supports used in industrial reactors are generally spherical or cylindrical pellets, with the catalytic agent deposited on the external surface or uniformly within the pellet.

The location of the catalytic material in the support can have a significant effect on catalyst performance, especially when diffusional resistances during reaction are important. For an isothermal reaction exhibiting positive-order kinetics, it is desirable to place the catalyst on the external surface of the support where the reaction concentration is the highest, while for negative-order kinetics (as in some concentration regimes of bimolecular Langmuir–Hinshelwood reactions), it is beneficial to locate the catalyst in the interior of the support where reactant concentration is lower (1). For exothermic reactions, even if they are of positive order, catalyst effectiveness can be increased by locating the catalytic agent inside the support, thus taking advantage of heat transport resistances (2).

The theory of optimal catalyst distribution has been developed even for the most general case of reacting systems: for any catalyst performance index (i.e., conversion, selectivity or yield) and for an arbitrary number of reactions, following arbitrary kinetics, occurring in a nonisothermal pellet, with finite external mass and heat transfer resistances, the optimal catalyst distribution is a Dirac delta function (3). It has also been shown that a step distribution of catalyst with step width about 5% of the pellet radius provides virtually the same results achieved by the optimal distribution (1). A step-type distribution is the true optimal distribution and not only an approximation, when the local catalyst concentration is considered to be bounded by an upper limit (4). Developments in the area of optimal distribution of catalyst have been reviewed recently (5).

A common method of catalyst preparation is by impregnation. A high-surface-area porous support is contacted with a liquid solution of active component. The active agent enters the porous support via capillary action and diffusion and adsorbs on the available surface sites. Supported platinum catalysts are usually prepared by contacting hexachloroplatinic acid with either a dry or solvent-filled support. When γ-Al_2O_3 pellets are impregnated with hexachloroplatinic acid, the resulting catalyst profile is of the eggshell type; i.e., the platinum is located in a thin shell at the support surface. Maatman (6) found that the platinum distribution could be made more uniform by the addition of various acids to the impregnating solution. Michalko (7) and others (cf. (8)) demonstrated that the presence of citric acid in the impregnation solution results in a subsurface band of platinum in alumina pellets. Shyr and Ernst (9) have shown that a variety of platinum profile shapes can be obtained by using different coimpregnants. In all of the above investigators, the preparation of the

[1] Current address: Department of Chemical and Biochemical Engineering, University College London, United Kingdom.

[2] To whom correspondence should be addressed. E-mail: avarma@darwin.cc.nd.edu

0021-9517/96 $12.00

TABLE 1

Physical Characteristics of γ-Al_2O_3 Pellets

Pellet length	0.32 cm
Pellet diameter	0.32 cm
Apparent density	1.73 g/cm^3
Surface area[a]	78.4 m^2/g
Average pore radius[a]	51.4 Å
Porosity	0.57

[a] Obtained by multipoint BET method.

supported platinum catalyst was based on the coimpregnation of hexachloroplatinic acid with another acid (usually citric acid). Lee and Aris (10) have provided an extensive review of catalyst preparation and have described models for various phases of single- and multicomponent impregnation.

Kulkarni *et al.* (11) used a simple model of plug flow into a single pore considering only two types of resistances at the liquid–solid interface: mass transfer and adsorption kinetics. Hegedus *et al.* (12) modeled competitive multicomponent adsorption on wet pellets by using adsorption constants determined from separate experiments. The model was used to predict the Rh distribution inside the pellet, when HF was used as the site blocking agent; diffusion constants were treated as adjustable parameters. Scelza *et al.* (13) used a similar model, but they treated not only the diffusion constants but also the adsorption constants as adjustable parameters. More detailed models have also been suggested, which take into account the chemistry of the solution–solid interface (14–16).

The present work addresses the preparation of step-type Pt/γ-Al_2O_3 pellets by impregnation. A diffusion–adsorption model which predicts satisfactorily the catalyst distribution inside the pellet is proposed. The parameters of the model, i.e., adsorption constants and effective diffusivities, were determined from separate experiments. In addition to coimpregnation, sequential impregnation was also used to prepare step-type catalyst pellets and yielded thinner step widths as compared with the former.

EXPERIMENTAL

Preparation of Step-Type Catalysts

Thin step-type Pt/γ-Al_2O_3 catalysts were prepared by coimpregnation and sequential impregnation techniques using citric acid as the competitive adsorbate. Harshaw–Filtrol AL-0104 cylindrical γ-Al_2O_3 pellets were used, and their physical characteristics are given in Table 1. Hexachloroplatinic acid solution was prepared by adding dihydrogen hexachloroplatinate (IV) (Aldrich A.C.S. grade) to deionized water. Citric acid (Fisher Scientific A.C.S. grade) was prepared in the same way. Before impregnation, the pellets were heated in air at 125°C and stored in a desiccator prior to use.

For *coimpregnation*, the pellets (about 4 g) were put in a flask and contacted with a mixture of citric acid and hexachloroplatinic acid (18 ml) for a given length of time. The flask was kept on a shaker (120 rpm) for the total impregnation period. The solution was then removed, and the pellets were washed with deionized water to remove the excess hexachloroplatinic acid from the exterior of the pellets. Two differential initial concentrations of hexachloroplatinic acid (0.00589 and 0.0117 *M*) and three different concentrations of citric acid (0.0556, 0.1111, 0.1667 *M*) were used, and the impregnation time was varied from 15 min to 2.5 h.

Sequential impregnation involved contacting the pellets in a similar manner as before with a solution of hexachloroplatinic acid (18 ml) for 15 min. The solution was removed and the pellets were washed with deionized water. They were then placed in a solution of citric acid (18 ml) for the desired impregnation duration. At the end of this period, the solution was removed and the pellets were washed with deionized water. Two different concentrations of hexachloroplatinic acid (0.00589 and 0.0117 *M*) and four different concentrations of citric acid (0.0556, 0.1111, 0.2222, 0.3333 *M*) were used, and the impregnation time (for the second step) was varied from 15 to 60 min.

At the end of the coimpregnation or the sequential impregnation period, the pellets were dried at 125°C for 18 h to immobilize both the citrate and the chloroplatinate ions. For visual observation the pellets were sectioned radially and dipped in boiling $SnCl_2$ solution. The location and width of the resulting platinum profile were determined by photographing the pellet and measuring the distances from the photographs. The pellets were calcined under a stream of oxygen from 25 to 500°C over a period of half an hour, followed by treatment in hydrogen for 1 h at 500°C. After this, the pellets were cooled in a nitrogen atmosphere.

Measurement of the platinum loading was performed by first crushing the pellets and extracting the platinum by a mixture of double-distilled HCl, HNO_3, and HF, in a ratio 3 : 3 : 1. The concentration of platinum in solution was then determined by ICP mass spectroscopy.

The catalyst dispersion was determined by measuring the platinum surface area by using hydrogen chemisorption according to the procedure described by Lemaitre *et al.* (17). Details of the pulse chemisorption setup used for the experiments are given elsewhere (18). The catalyst in powder form was first treated in hydrogen at 450°C for 1 h and after cooling to 25°C, was subjected to an oxidation–reduction–oxidation cycle, to obtain reproducible results.

Determination of Equilibrium Adsorption Constants and Adsorption Rate Constants

The single-component equilibrium adsorption parameters were determined by contacting a known amount of γ-Al_2O_3 that was ball-milled to 20 μm and dried at 125°C for 8 h, with a known concentration of citric acid or hexachloroplatinic acid. The slurries were kept in a shaker during the impregnation period. They were then filtered and the filtrate concentration was determined by either atomic absorption spectroscopy for hexachloroplatinic acid or sodium hydroxide titration (using a Fisher Accumet Model 805MP pH meter) for citric acid. The amount of solute adsorbed on γ-Al_2O_3 was determined from the difference in solution concentration before and after impregnation.

Adsorption rate constants were measured by transient adsorption experiments. In each experiment, approximately 30 g powdered γ-Al_2O_3 was added to 200 ml impregnating solution of known concentration. The slurry was kept in a shaker at all times. At selected time intervals, 0.1 ml of the slurry was removed and immediately filtered. The filtrate concentration was then measured by the techniques described previously. The adsorption rate constants were determined by fitting the transient data.

Some transient multicomponent adsorption experiments which mimic the sequential impregnation of γ-Al_2O_3 pellets were also carried out. For these, γ-Al_2O_3 powder was first impregnated with a solution of hexachloroplatinic acid for 1 h and the slurry was then centrifuged to separate the solid from the liquid. Afterward, the liquid phase was decanted off, and citric acid was added to the solid for further impregnation, which was allowed to progress for 1 h.

Effective Diffusivity Measurement

Effective diffusivities of citric and hexachloroplatinic acid were measured under well-mixed conditions in a spinning basket and a packed-bed apparatus. The first consisted of four stainless-steel baskets mounted on a common axis that was rotated by a stirring motor. The baskets were placed in a closed vessel which contained the fluid. The fluid was stirred by a magnetic spin bar rotating counter to the baskets. This kept the liquid flowing over the pellet surface maintaining high interphase mass transfer. The packed-bed apparatus consisted of a quartz tube containing the pellets. A peristaltic pump recycled the bulk fluid over the pellets to achieve good mass transfer. More details about the effective diffusivity measurements have been reported elsewhere (19). Interphase mass transfer between the liquid and the solid phase for both setups was much faster than intraphase mass transfer (19) and therefore the concentration of solute in the pore fluid at the pellet surface was equal to the bulk fluid concentration.

To decouple diffusion from adsorption/desorption phenomena, the pellets were first placed in a high-concentration solution of citric acid or hexachloroplatinic acid for several days to achieve equilibrium between the adsorbed phase and the bulk phase. The pellets were then loaded in either apparatus, bulk fluid of a different (but still high) concentration was added, and the units were turned on. At various time intervals, the bulk fluid was sampled and the concentration was measured. All experiments were performed at room temperature.

SINGLE-COMPONENT EQUILIBRIUM AND TRANSIENT ADSORPTION RESULTS

If adsorption of citric acid or hexachloroplatinic acid is described by the Langmuir model, the rate of adsorption in the absence of mass transfer resistance is given by

$$\frac{dn}{dt} = k^+ c(n_s - n) - k^- n. \qquad [1]$$

At equilibrium, the amount adsorbed can be calculated by setting the transient term equal to zero, thus giving the Langmuir adsorption isotherm

$$n_e = \frac{Kc_e n_s}{1 + Kc_e}, \qquad [2]$$

where $K = k^+/k^-$ is the equilibrium adsorption constant. Note that c_e is the solution concentration and n_e the corresponding surface concentration at equilibrium. The quantity n_e is calculated from the difference between the initial and equilibrium solution concentrations. It was found that the above isotherm fitted both citric acid and hexachloroplatinic acid adsorption data well. By using a nonlinear least-squares algorithm (Levenberg–Marquardt), the equilibrium adsorption constant, K, and the surface saturation coverage, n_s, were obtained for each component. During the adsorption experiments for both citric acid and hexachloroplatinic acid, it was observed that the fluid concentration changed relatively little with time after approximately 60 min.

From the equilibrium data, hexachloroplatinic acid was found to have a surface saturation coverage of 121 μmol/g (1.55 μmol/m^2) and an equlibrium adsorption constant of 606 liter/mol. For citric acid, the surface saturation coverage was found to be 209 μmol/g (2.68 μmol/m^2) and the equilibrium constant was 19530 liter/mol. Figure 1 shows the experimental results of the equilibrium experiments along with the predicted isotherms using the calculated parameters for hexachloroplatinic acid and citric acid, respectively. It is worth noting that Freundlich isotherms could not describe the adsorption of either the hexachloroplatinic acid or citric acid on the support.

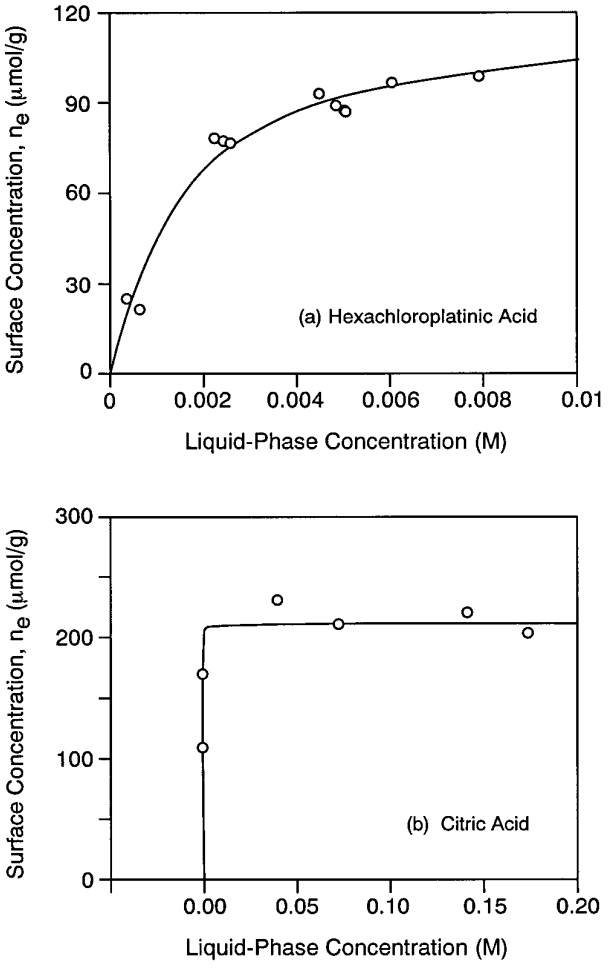

FIG. 1. Equilibrium adsorption isotherm of (a) hexachloroplatinic acid (c_{bo} = 0.01287 *M*) and (b) citric acid (c_{bo} = 0.00544 *M*) on γ-Al_2O_3 powder and the fitted Langmuir adsorption models.

For hexachloroplatinic acid, the surface saturation coverage reported in the literature ranges from 110 to 290 μmol/g, while the value of adsorption equilibrium constant varies from 110 to 31000 l/mol (see Table 2). The values obtained in this work are within the above ranges. The large range of the adsorption equilibrium constant, though, makes the comparison more difficult. Note that if the surface saturation coverage is based on the surface area of the support, the above range of values becomes 0.73 to 1.5 μmol/m^2, while the saturation coverage obtained in this study is 1.55 μmol/m^2.

Data for citric acid adsorption are relatively scarce (see Table 3). Shyr and Ernst (9) reported that even though the adsorption isotherm showed a saturation behavior, a Langmuir adsorption model did not fit their data obtained for citric acid on γ-Al_2O_3. However, Engels *et al.* (20) fitted their data with a Langmuir model and found the equilibrium adsorption constant to be 2070 liter/mol. This value is smaller than that obtained in the present study, and this may be because it was calculated by linearizing the adsorption equation. In this case, K is obtained from the line intercept. For large K values, the intercept being close to zero renders this method unreliable.

The surface saturation coverage reported by Shyr and Ernst (9) was 215 μmol/g (1.43 μmol/m^2). Jianguo *et al.* (21) fitted adsorption data of citric acid on η-Al_2O_3 and found that the saturation coverage was 820 μmol/g (3.35 μmol/m^2). Engles *et al.* (20) obtained a value of 444 μmol/g (2.02 μmol/m^2). In the present study, the equilibrium data gave a value of 209 μmol/g (2.68 μmol/m^2). The differences among the various studies may lie partly in the duration of impregnation.

When comparing the adsorption data from various γ-Al_2O_3 supports, caution should be exercised due to the variances that may be present in the supports. Jiratova (22) demonstrated that the isoelectric point (the pH where no adsorption occurs) of alumina varies strongly with trace impurities in the solid and the value of isoelectric point influences the amount of adsorption that occurs for a given solution pH. Furthermore, the solution pH also greatly affects the adsorption properties of a given γ-Al_2O_3 sample (23) and in turn depends on the hexachloroplatinic acid concentration. In addition, even for a specific concentration of hexachloroplatinic acid, solely the amount of γ-Al_2O_3 added can alter the solution pH; i.e., the pH depends on the ratio of solution volume to mass of alumina (V/G) (24). These investigators have shown that when alumina is added gradually to a solution, its pH changes and approaches the isoelectric point of the oxide. Considering the fact that the data shown in Table 2 were obtained over a large range of V/G values (5–80 ml/g) and with different alumina samples, the large range of adsorption parameters obtained may be justifiable.

Once the equilibrium adsorption constant and surface saturation coverage are known, the only parameter in the Langmuir adsorption model remaining to be calculated is the adsorption rate coefficient k^+. For this purpose, a transient adsorption equation based on measurable quantities is developed as follows.

The amount of solute adsorbed, n, can be calculated by knowing the solution concentration at a particular time t:

$$n(t) = \frac{V}{G}[c_0 - c(t)]. \qquad [3]$$

Substituting Eq. [3] into [1], the concentration of bulk solution as a function of time is obtained:

$$-\frac{dc}{dt} = k^+c^2 + \left(k^- + \frac{G}{V}k^+n_s - k^+c_0\right)c - k^-c_0. \qquad [4]$$

TABLE 2

Values of Adsorption Parameters of Hexachloroplatinic Acid on γ-Al_2O_3 in Water Solution

Area (m^2/g)	K (liter/mol)	k^+ (liter/mol·s)	n_s (μmol/g)	n_s (μmol/m^2)	t_e (h)	Reference
177	459	1.21	265	1.50	3–8	(35)
150	1330		110	0.73	2	(9)
170	31000		140	0.82	6	(34)
245			275	1.12	6	(21)[a]
	7200	1.70				(13)
190	1550		151	0.79	0.3	(36)
195	110	0.18	290	1.48	2	(37)
227			205	0.90	1	(23)
78	606	2.46	121	1.55	1.5	This study

[a] Solid was η-Al_2O_3.

Equation [4] is then fitted to transient adsorption data to determine k^+. For hexachloroplatinic acid, its value was calculated to be 2.46 liter/mol·s, while for citric acid, it was 7.97 liter/mol·s. Values of adsorption rate constant for hexachloroplatinic acid reported in the literature (see Table 2) vary to some extent. No constants have been reported for the transient adsorption of citric acid.

Figure 2 shows experimental results from transient experiments along with the model predictions for both hexachloroplatinic acid and citric acid. It should be noted that the adsorption rate for citric acid was extremely fast.

MULTICOMPONENT EQUILIBRIUM AND TRANSIENT ADSORPTION RESULTS

When more than one adsorbate are present in solution, competition between them for adsorption sites must be taken into account. For this, initially a purely competitive model (i.e., no interactions between the adsorbates either on the support surface or in the fluid phase) was formulated. The adsorption equation of the ith component in a two-component system is given by

$$\frac{dn_i}{dt} = k^+_{mi} c_i (n_{ms} - \lambda_i n_i - \lambda_j n_j) - k^-_{mi} n_i. \qquad [5]$$

The multicomponent expression should collapse into the single component expression (Eq. [1]) when only one adsorbate is present; therefore the ratio n_{ms}/λ_i should equal the single-component surface saturation coverage, n_{si}, and $\lambda_i k^+_{mi}$ the single-component adsorption rate constant, k^+_i. Also, the ratio λ_j/λ_i should equal the ratio of the single-component saturation coverages n_{si}/n_{sj}, and k^-_{mi} the single component desorption rate constant, k^-_i. Thus, Eq. [5] can be rearranged as

$$\frac{dn_i}{dt} = k^+_i c_i \left(n_{si} - n_i - \frac{n_{si}}{n_{sj}} n_j \right) - k^-_i n_i. \qquad [6]$$

This model, however, was unable to describe the multicom-

TABLE 3

Values of Adsorption Parameters of Citric Acid on γ-Al_2O_3 in Water Solution

Area (m^2/g)	K (liter/mol)	k^+ (liter/mol·s)	n_s (μmol/g)	n_s (μmol/m^2)	t_e (h)	Reference
150			215	1.43	2	(9)
245			820	3.35	6	(21)[a]
220	2070		444	2.02	2	(20)
78	19530	7.97	209	2.68	1.5	This study

[a] Solid was η-Al_2O_3.

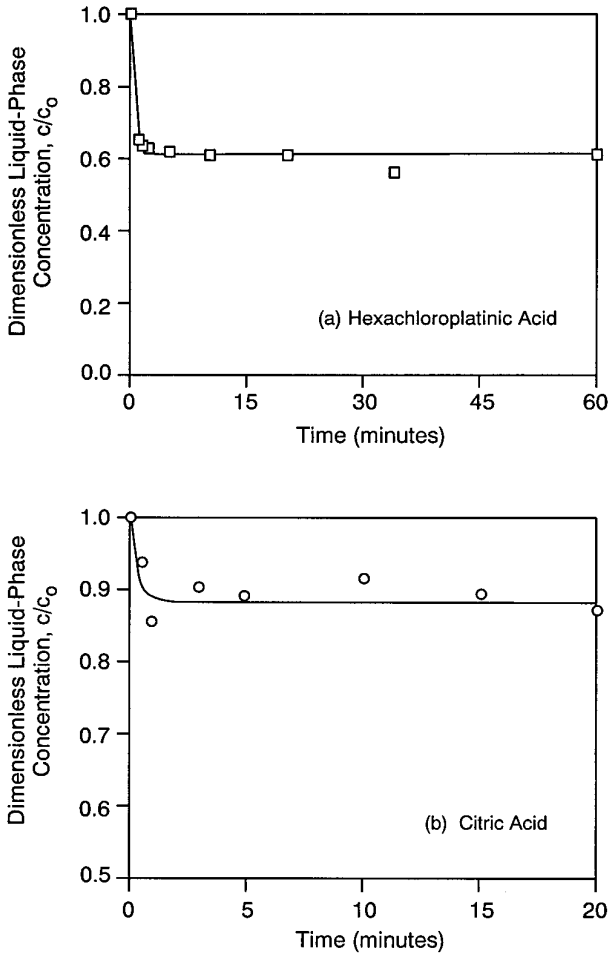

FIG. 2. Transient adsorption during impregnation of γ-Al_2O_3 powder with (a) hexachloroplatinic acid (G/V = 50.2 g/liter) and (b) citric acid (G/V = 3.12 g/liter) and fitted Langmuir adsorption models.

ponent experimental data satisfactorily. For this reason, a model which accounted for *solution effects* for hexachloroplatinic acid and *steric hinderances effects* for citric acid was formulated.

In the multicomponent adsorption experiments, the γ-Al_2O_3 initially contained adsorbed hexachloroplatinic acid. The amount of hexachloroplatinic acid desorbed when γ-Al_2O_3 was subsequently placed in the citric acid solution was in excess of that predicted by the single-component model but less than that predicted from the purely competitive model. Also, the initial desorption rate of hexachloroplatinic acid was larger than that computed from both models, suggesting that its desorption is enhanced by the presence of citric acid in solution. This was accounted for by introducing an additional desorption term in the single-component adsorption expression as follows:

$$\frac{dn_1}{dt} = k_1^+ c_1(n_{s1} - n_1) - k_1^- n_1 - k_1^{sol} c_2 n_1. \qquad [7]$$

The amount of citric acid adsorbed during the multicomponent experiments was less than the amount which would be expected based on a purely competitive model described by Eq. [6] for citric acid and Eq. [7] for hexachloroplatinic acid. Such behavior could be due to steric hinderances provided by the platinum adsorbed on the surface of γ-Al_2O_3. This was accounted for by introducing a new equilibrium adsorption constant K_2^{st}, due to steric hinderances,

$$\frac{dn_2}{dt} = k_2^+ c_2(n_{s2} - n_2 - K_2^{st} n_1) - k_2^- n_2. \qquad [8]$$

By comparing Eq. [8] with [6], it can easily be seen that K_2^{st} for a purely competitive model corresponds to n_{s2}/n_{s1}; thus it is the ratio of the stoichiometric factors (λ_1/λ_2) for hexachloroplatinic acid and citric acid adsorption equilibria. The equilibrium expressions including the new terms are

$$n_{1e} = \frac{K_1 c_{1e} n_{sl}}{1 + K_1 c_{1e} + K_1^{sol} c_{2e}} \qquad [9]$$

$$n_{2e} = \frac{K_2 c_{2e}}{1 + K_2 c_{2e}} (n_{s2} - K_2^{st} n_{1e}). \qquad [10]$$

The two new parameters in the multicomponent equilibrium model expressed by Eqs. [9] and [10], namely K_1^{sol} and K_2^{st}, were determined by fitting the equilibrium data to be 735 and 3.18 liter/mol, respectively.

In the kinetic expressions (Eqs. [7] and [8]), once the equilibrium constants (i.e., K_1 and K_2) have been obtained, only one parameter for each component needs to be determined (i.e., k_1^+ and k_2^+). The values of the desorption rate constants can then be calculated from the equilibrium constants.

Figure 3 shows the transient multicomponent adsorption experimental data for hexachloroplatinic and citric acids along with the model curves. It was found that use of the single-component adsorption rate constant for hexachloroplatinic acid (2.46 liter/mol·s) was satisfactory also in the transient multicomponent adsorption; however, the adsorption rate constant of citric acid had to be lowered to 0.2 liter/mol·s in order to achieve the best fit. Note that in Fig. 3a, the model curve is based on the adsorption rate constant which was determined by fitting the data of a *different* experiment. Thus the model predictions of the liquid-phase concentrations are satisfactory. In the same figure, the hexachloroplatinic acid concentration calculated from the model shows an initial maximum and then it declines to the steady-state value. The reason for this is that the concentration of citric acid decreases with time as

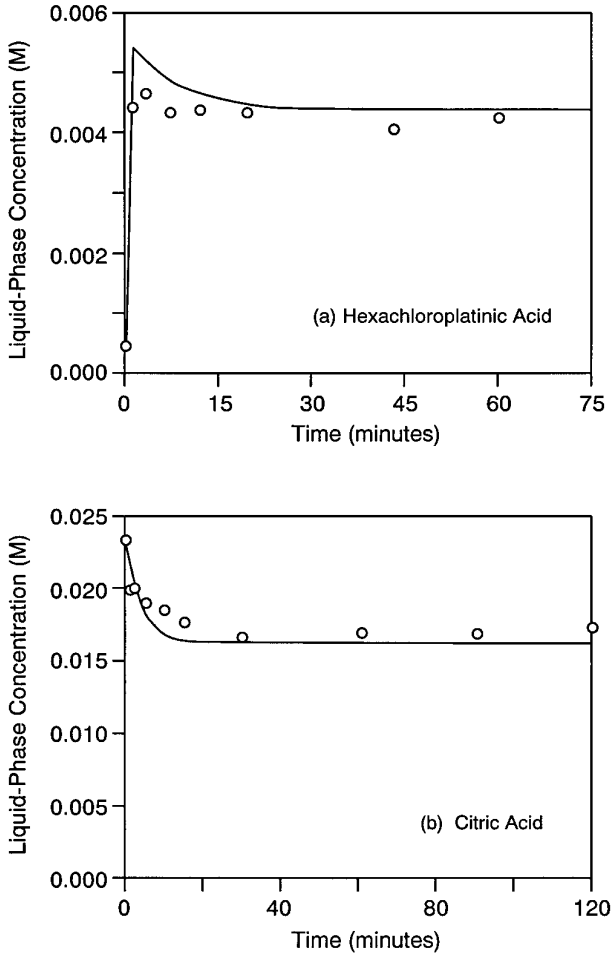

FIG. 3. Transient multicomponent adsorption on γ-Al_2O_3 powder with model predictions of liquid-phase concentration as a function of time for (a) hexachloroplatinic acid and (b) citric acid.

it adsorbs on γ-Al_2O_3. At the onset of citric acid impregnation, the fluid-phase concentration of citric acid is relatively high, thus causing some desorption of the platinum from the γ-Al_2O_3 support. As the solution concentration of citric acid declines due to adsorption, there is a readsorption of platinum, which decreases the liquid-phase concentration of hexachloroplatinic acid, as also observed in the experimental data.

As noted earlier, more detailed models which take into account electrokinetic and ionic dissociation effects have been suggested in the literature (cf. (14–16)). They include a more realistic description of the surface chemistry at the expense of model complexity. In the present study, it was intended to keep the model simple such that kinetics and equilibria for multicomponent systems collapse into the appropriate single-component expressions in the limit as concentration of one component goes to zero.

EFFECTIVE DIFFUSIVITIES

The equation governing the transient transport and adsorption of a solute in a porous solid of cylindrical geometry, initially filled with solvent, is

$$\varepsilon \frac{\partial c_p}{\partial t} + \rho_s \frac{\partial n}{\partial t} = D_e \left\{ \frac{\partial^2 c_p}{\partial x^2} + \frac{1}{r} \frac{\partial}{\partial r} \left(r \frac{\partial c_p}{\partial r} \right) \right\}. \qquad [11]$$

Since the interphase mass transport resistances during the effective diffusivity measurement experiments are negligible, the boundary conditions are

$$c_p(x, R) = c_p(\pm L/2, r) = c_b(t) \qquad [12a]$$

$$\left. \frac{\partial c_p}{\partial x} \right|_{x=0} = \left. \frac{\partial c_p}{\partial r} \right|_{r=0} = 0. \qquad [12b]$$

Absorbate concentration in the bulk solution (assumed to be well mixed) changes as the solute diffuses into and adsorbs on the support, because the bulk reservoir is finite. The change of bulk solute concentration is given by

$$V \frac{dc_b}{dt} = -N_p D_e 4\pi \left\{ R \int_0^{L/2} \left. \frac{\partial c_p}{\partial r} \right|_{r=R} dx + \int_0^R r \left. \frac{\partial c_p}{\partial x} \right|_{x=L/2} dr \right\}. \qquad [13]$$

In Langmuir adsorption, surface concentration of adsorbate does not change appreciably once the fluid concentration reaches a sufficiently high value. By keeping both the pore and the bulk fluid in this concentration range, adsorption/desorption do not occur and hence are decoupled from diffusion, thus simplifying the diffusion–adsorption Eq. [11] (i.e., $\partial n/\partial t = 0$). To ensure that no further adsorption could occur, equilibrium was established for the pellets prior to their use in diffusivity experiments.

Since there was some occluded liquid between the pellets when they were first loaded into the apparatus, the bulk fluid concentration was altered from its initial concentration, which had to be accounted for. To calculate the correct initial value, a material balance was performed after the pellets were equilibrated with the bulk fluid. The corrected initial concentration is given by

$$c_{bo} = \frac{c_{b\infty}(V + N_p \varepsilon \pi R^2 L) - N_p \varepsilon \pi R^2 L c_{po}}{V}. \qquad [14]$$

Effective diffusivities were determined by solving Eqs. [11] and [13], using the value of D_e as the fitting parameter. One octant of the pellet was divided into a grid containing

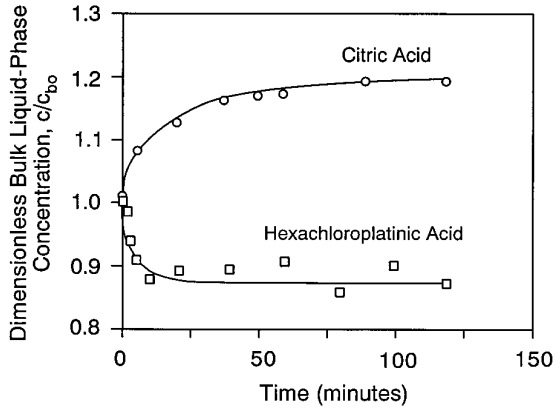

FIG. 4. Effective diffusivity measurements of hexachloroplatinic acid and citric acid with fitted model predictions. Experimental conditions for (a) citric acid: $c_{po} = 2.78\ M$, $c_{bo} = 0.229\ M$ and (b) hexachloroplatinic acid: $c_{po} = 0.0283\ M$, $c_{bo} = 0.1071\ M$.

10 points in the axial and radial directions. Orthogonal collocation (25) was used for the spatial variables, while Gear's method (IMSL subroutine DGEAR) was used to solve for the time dependence of the concentration at each collocation point and the concentration in the bulk fluid.

Figure 4 shows the results for one citric acid (spinning basket) and one hexachloroplatinic acid (packed bed) effective diffusivity runs. D_e was determined to be 0.96×10^{-6} cm^2/s for citric acid and 3.12×10^{-6} cm^2/s for hexachloroplatinic acid. The molecular diffusivity, D_m, of citric acid in water at 25°C and 0.1 M concentration is 6.61×10^{-6} cm^2/s (26). With this value and the effective diffusivity value determined experimentally, the tortuosity factor $\tau = \varepsilon D_m/D_e$ is 3.9, which is within the range 2–7 of typical tortuosity factors (27). The molecular diffusivity of hexachloroplatinic acid was not available in the literature. Scelza *et al.* (13) report an effective diffusivity of 2.25×10^{-5} cm^2/s for hexachloroplatinic acid in γ-Al_2O_3 particles. This value is higher than that reported in the present work. This may be due to the fact that they calculated *both* effective diffusivities *and* adsorption rate constants by fitting a diffusion–adsorption model with experimental data obtained under conditions where both diffusion and adsorption were present. Santacesaria et al. (28), by fitting the diffusion-controlled hexachloroplatinic acid impregnation of γ-Al_2O_3 pellets with an unreacted-core shrinking model, calculated an effective diffusivity of 3.55×10^{-6} cm^2/s, which agrees well with this work.

DIFFUSION-ADSORPTION MODEL

Model Formulation

For multicomponent impregnation of cylindrical pellets in a finite reservoir of solution, the material balance inside the pellet for species i is given by the multicomponent version of Eq. [11]:

$$\varepsilon \frac{\partial c_{p,i}}{\partial t} + \rho_s \frac{\partial n_i}{\partial t} = D_{e,i}\left\{\frac{\partial^2 c_{p,i}}{\partial x^2} + \frac{1}{r}\frac{\partial}{\partial r}\left(r\frac{\partial c_{p,i}}{\partial r}\right)\right\}. \quad [15]$$

The multicomponent adsorption kinetics (Eqs. [7] and [8]) were used to describe the adsorption rates, $\partial n_i/\partial t$. Even though these kinetics were obtained under conditions of sequential impregnation, the results were utilized also for describing the coimpregnation of γ-Al_2O_3 pellets. The depletion of species i in the bulk solution is given by

$$V\frac{dc_{b,i}}{dt} = -N_p D_{e,i} 4\pi \left\{R\int_0^{L/2}\left.\frac{\partial c_{p,i}}{\partial r}\right|_{r=R} dx + \int_0^R r\left.\frac{\partial c_{p,i}}{\partial x}\right|_{x=L/2} dr\right\}. \quad [16]$$

The boundary conditions are

$$c_{p,i}(x, R) = c_{p,i}(\pm L/2, r) = c_{b,i}(t) \quad [17a]$$

$$\left.\frac{\partial c_{p,i}}{\partial x}\right|_{x=0} = \left.\frac{\partial c_{p,i}}{\partial r}\right|_{r=0} = 0. \quad [17b]$$

For citric acid, the initial conditions for both types of impregnation are

$$c_{b,2} = c_{bo,2} \quad \text{at } t = 0 \quad [18a]$$

$$c_{p,2} = n_2 = 0 \quad (0 \le r \le R, 0 \le x \le L/2) \quad \text{at } t = 0. \quad [18b]$$

In coimpregnation and in the first impregnation (where only hexachloroplatinic acid is present) of the pellets during sequential impregnation, initial conditions for hexachloroplatinic acid are similar to those described by Eqs. [18]. In sequential impregnation, after the pellets are removed from the hexachloroplatinic acid and placed in the citric acid solution, the new initial conditions for hexachloroplatinic acid are

$$c_{b,1} = 0 \quad \text{at } t = 0 \quad [19a]$$

$$c_{p,1}(r, x) = c^*_{p,1}(r, x); \quad n_1(r, x) = n^*_1(r, x) \quad \text{at } t = 0, \quad [19b]$$

where $c^*_{p,1}(r, x)$ and $n^*_1(r, x)$ are the pore-fluid and surface concentrations at the end of the first impregnation.

Note that even though during the experiments the pellets were initially dry, thus some of the solution entered by imbibition, Eq. [15] assumes that the pores of the pellet are initially filled with solvent. Lee and Aris (10) showed by numerical calculations that for the impregnation of γ-

Al_2O_3 pellets with hexachloroplatinic acid in which the pore-filling time was approximately 20 s, there was no noticeable difference between the platinum distributions in solvent-filled and dry supports when the impregnation period lasted 5 min or more. The reason for this is the short pore-filling time of the pellets. During the pore-filling stage, hexachloroplatinic acid adsorbs near the external surface of the pellet; thus the pores become filled with pure solvent. In our experiments the average pore-filling time was 12 s, while the impregnation periods varied from 15 min to 2.5 h; thus using a solvent-filled pellet to describe the impregnation of dry pellets does not induce any significant error.

Citric acid and hexachloroplatinic acid adsorb strongly on γ-Al_2O_3. Due to the strong precursor–support interaction, redistribution during the washing and drying steps is unlikely, and the final distribution of active phase is determined mainly in the impregnation step (cf. (29)).

Numerical Solution

The partial differential equations [15]–[19] describing the multicomponent diffusion and adsorption in a finite cylinder were solved by dividing one octant of the pellet into a region of $N \times N$ grid points (recall from Table 1 that pellet $L/2R = 1$) extending from the pellet center to the radial and axial surfaces. The spatial derivatives were solved using the finite difference technique with central differencing (25). This reduced Eqs. [15] and [16] to a system of coupled nonlinear ordinary differential equations (ODEs), with time as the independent variable.

A sixth-order Runge–Kutta algorithm (IMSL subroutine DVERK) was used to integrate the equations. It was found that to achieve a reasonable spatial resolution a large number of grid points was required ($N = 50$), resulting in large computational times. To alleviate this problem one-dimensional geometry (i.e., sphere) was used. The external geometric surface area of a cylinder with length equal to its diameter is 1.5 times larger than that of a sphere with the same diameter. So, to have the equivalent geometric surface area, the number of spherical pellets, M_p, should be 1.5 times the number of cylindrical ones, N_p. By using this factor, there is no difference between the mass of the supports if the same pellet density is used. The dimensionless multicomponent equations describing the impregnation of a sphere are

$$\varepsilon \frac{\partial c_{p,i}}{\partial t} + \rho_s \frac{\partial n_i}{\partial t} = D_{e,i} \left\{ \frac{1}{r^2} \frac{\partial}{\partial r} \left(r^2 \frac{\partial c_{p,i}}{\partial r} \right) \right\} \qquad [20]$$

$$V \frac{dc_{b,i}}{dt} = -M_p D_{e,i} 4\pi R^2 \left\{ \frac{\partial c_{p,i}}{\partial r} \bigg|_{r=R} \right\}. \qquad [21]$$

Using the above equations for the model the reduction in computational time was substantial. The average error in the pore-fluid concentration predictions, using the spherical geometry equations (Eqs. [20], [21]) as compared to the cylindrical geometry (Eqs. [15], [16]), was typically less than 10%.

EXPERIMENTAL OBSERVATIONS AND COMPARISON WITH MODEL PREDICTIONS

The diffusion–adsorption model described previously predicted successfully the effects of the various impregnation parameters on the platinum distribution within the pellet. The cross sections of pellets prepared by sequential and coimpregnation techniques are shown in Fig. 5. The dark rings in Figs. 5a–5i are the platinum catalyst, while the lighter portion is the γ-Al_2O_3 support. For comparison, eggshell, egg-yolk, and uniform pellets are also shown in Figs. 5j–5l.

For both types of impregnations, the platinum band was located deeper inside the pellet for higher initial critic acid concentration (compare Figs. 5b–5c, 5e–5f, 5h–5i). In addition, higher impregnation time forced the platinum to move closer to the pellet center, since the citric acid could diffuse further inside the pellet and displace the adsorbed platinum (compare Figs. 5a–5b, 5d–5e, 5g–5h). Similar effects during coimpregnation of alumina pellets with hexachloroplatinic and citric acid were also observed by Becker and Nuttall (8).

The initial hexachloroplatinic acid concentration did not have any noticeable effect on the catalyst location; however, it resulted in catalysts with higher loading and somewhat larger bandwidths (compare Figs. 5a–5d, 5b–5e, 5c–5f). The bandwidth was also influenced by impregnation time, owing primarily to geometric effects. Since the diameter of the ring, where the platinum was located, decreased with time, its width increased to accommodate the deposited metal (compare Figs. 5a–5b, 5d–5e, 5g–5h). In general, for the same impregnation time and adsorbate concentrations, a similar penetration depth was achieved by both types of impregnations (compare Figs. 5a–5g, 5b–5h), but the bandwidth was smaller (as small as 50 μm) when using sequential impregnation.

In coimpregnation experiments the platinum loading of the samples was affected not only by the initial hexachloroplatinic acid concentration but also to a smaller extent, by the citric acid concentration. The loading decreased with higher initial concentration of citric acid. However, during sequential impregnation, the platinum loading of the pellets depended primarily on the conditions of the first impregnation step. It could be kept approximately constant by using the same hexachloroplatinic acid concentration for the first step. The fact that citric acid concentration did not affect the platinum loading of pellets prepared by sequential impregnation indicates a different mode of action: in coimpregna-

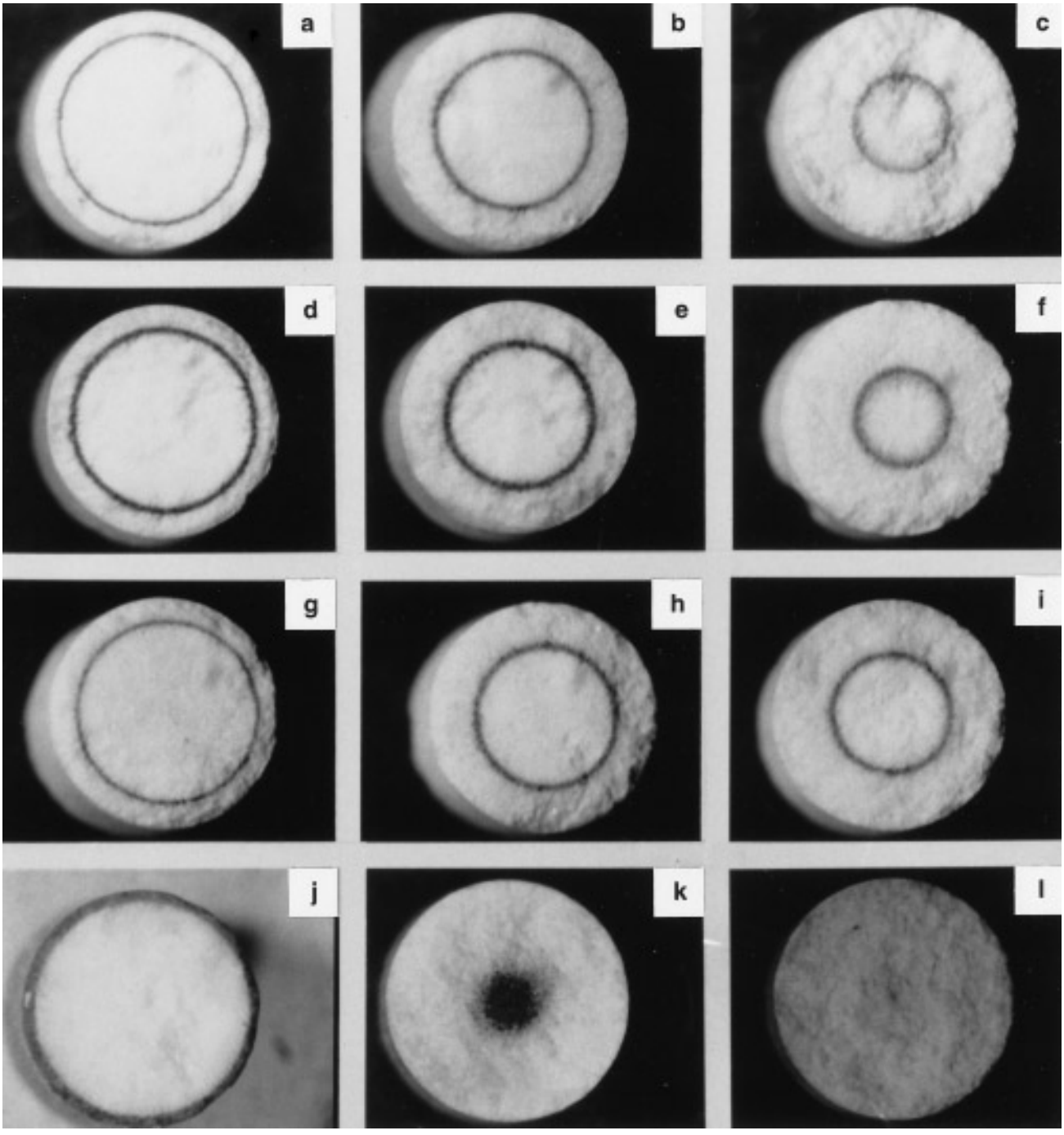

FIG. 5. Step-type platinum catalysts prepared by sequential impregnation (a) 0.00589 *M* hexachloroplatinic acid (15 min), 0.1111 *M* citric acid (15 min); (b) 0.00589 *M* hexachloroplatinic acid (15 min), 0.1111 *M* citric acid (60 min); (c) 0.00589 *M* hexachloroplatinic acid (15 min), 0.3333 *M* citric acid (60 min); (d) 0.0117 *M* hexachloroplatinic acid (15 min), 0.1111 *M* citric acid (15 min); (e) 0.0117 *M* hexachloroplatinic acid (15 min), 0.1111 *M* citric acid (60 min); (f) 0.0117 *M* hexachloroplatinic acid (15 min), 0.3333 *M* citric acid (60 min) and coimpregnation (g) 0.00589 *M* hexachloroplatinic acid and 0.1111 *M* citric acid (15 min); (h) 0.00589 *M* hexachloroplatinic acid and 0.1111 *M* citric acid (60 min); (i) 0.00589 *M* hexachloroplatinic acid and 0.1667 *M* citric acid (60 min); (j) 0.0117 *M* hexachloroplatinic acid (15 min); (k) 0.0117 *M* hexachloroplatinic acid and 0.1667 *M* citric acid (3 h); (l) 0.0117 *M* hexachloroplatinic acid and 0.1667 *M* citric acid (10 h).

tion it competes with hexachloroplatinic acid for adsorption on the support, while in sequential impregnation it enhances the desorption of adsorbed platinum. The platinum loading of the pellets as measured by ICP mass spectroscopy was in the range 0.1–0.4 wt%, depending on the initial hexachloroplatinic acid concentration.

The eggshell distribution (Fig. 5j) was prepared by impregnating the pellet in a solution of hexachloroplatinic acid alone. The egg-yolk distribution (Fig. 5k) could be achieved by both sequential and coimpregnation, provided that the impregnation periods were sufficiently long, while the uniform distribution (Fig. 5l) was obtained using the coimpregnation method. Note that the difference in the preparation procedure of pellets depicted in Fig. 5k and Fig. 5l is only the impregnation duration. Thus, for short coimpregnation time an egg-white deposition is obtained, while for longer impregnation periods egg-yolk and ultimately uniform distributions are attained. Catalyst dispersion of the pellets, including both step and uniform distributions, as measured by hydrogen chemisorption, ranged between 60 and 70%. Hence, for pellets with relatively low platinum loadings as considered in this study, the dispersion is virtually unaltered when concentrating the metal in a thin step-type distribution. These dispersion values are within the range reported for typical Pt/γ-Al_2O_3 catalysts (cf. (30, 31)).

Figures 6 and 7 show the predicted dimensionless platinum surface concentration profiles, along with the experimentally measured platinum band positions denoted by the shadowed regions for the sequential and coimpregnation studies, respectively. The numbers on the bands give the impregnation time (for sequential impregnation it is the time in the citric acid solution). The penetration depth of platinum predicted by the model for both impregnation techniques is greater with increasing impregnation time, as also observed experimentally. In addition, the model is able to predict that the bandwidths are broader for the coimpregnation than for the sequential impregnation technique (compare Figs. 6b and 7b), as well as the fact that bandwidth increases with impregnation time. Note that the model predicts that some adsorbed platinum extends from the peak to the pellet surface, with coimpregnation exhibiting more platinum in that region than sequential impregnation. Our pellets showed evidence (i.e., light-gray color) of small amounts of platinum deposited between the step distribution and the pellet external surface. This was also observed previously by Kunimori *et al.* (32) in the preparation of similar catalysts using hexachloroplatinic acid and citric acid.

Figure 8 compares model predictions for the platinum peak location with experimental data, for various citric acid concentrations and impregnation time. The model agrees well with the experimental data and demonstrates that by increasing citric acid concentration for both impregnation techniques, the platinum band moves deeper within the pellet. The maximum difference between the experimental and the theoretical peak locations is less than 8% of the pellet radius. An interesting feature is that the model predictions are closer to the experimental data for deeper band penetrations (cf. Fig. 8b). This was also observed by Hegedus *et al.* (12) in the coimpregnation of γ-Al_2O_3 pellets with a rhodium complex and hydrofluoric acid.

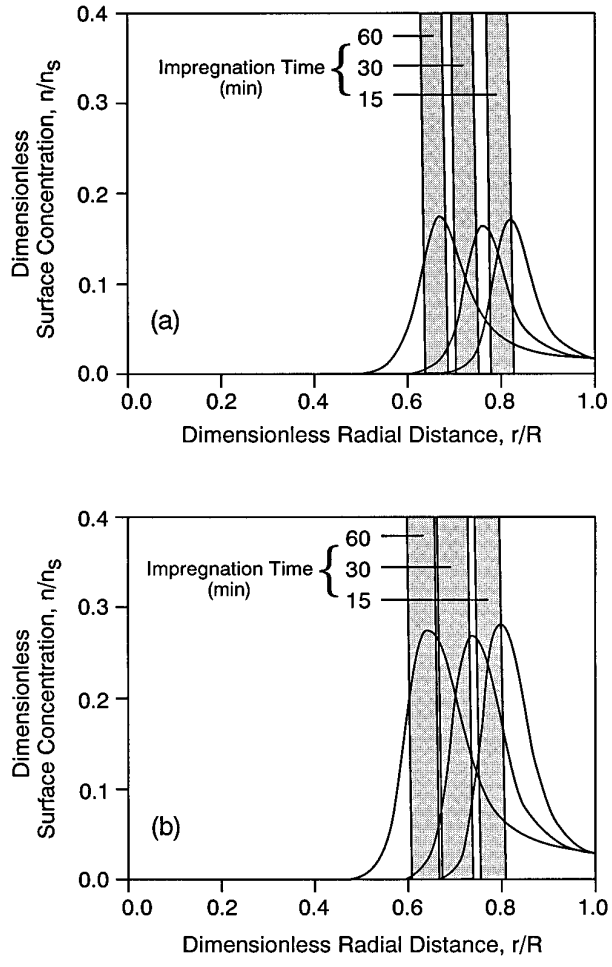

FIG. 6. Comparison of model predictions and experimental measurements of the surface concentration profiles of platinum for sequential impregnation with 0.1111 *M* citric acid, (a) 0.00589 *M* hexachloroplatinic acid, (b) 0.0117 *M* hexachloroplatinic acid. The shaded bands indicate the experimentally measured platinum step positions, and the numbers on the bands give the impregnation time in the citric acid solution.

CONCLUDING REMARKS

Since the adsorption and diffusion parameters were not adjusted to fit the diffusion–adsorption model, accord of the model with experimental data as shown in Figs. 6–8 appears to be satisfactory. These parameters were determined from separate experiments in which diffusion and

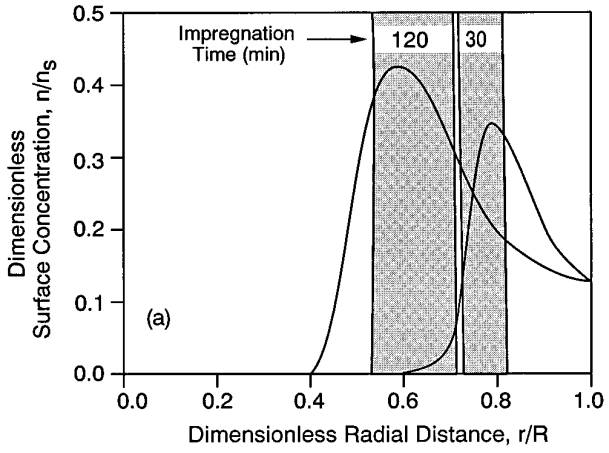

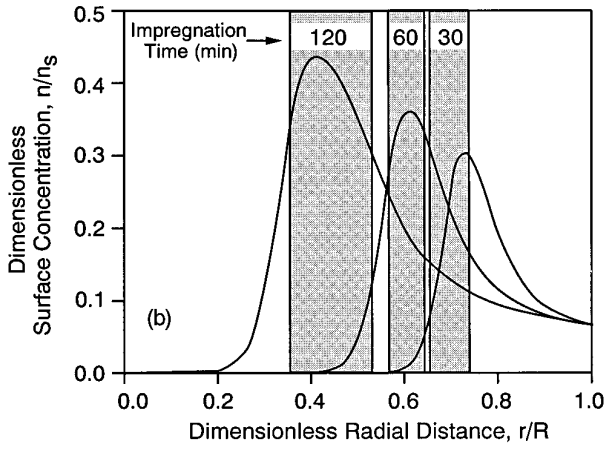

FIG. 7. Comparison of model predictions and experimental measurements of the surface concentration profiles of platinum for coimpregnation with 0.0117 *M* hexachloroplatinic acid, (a) 0.0556 *M* citric acid, (b) 0.1111 *M* citric acid. The shaded bands indicate the experimentally measured platinum step positions, and the numbers on the bands give the impregnation time.

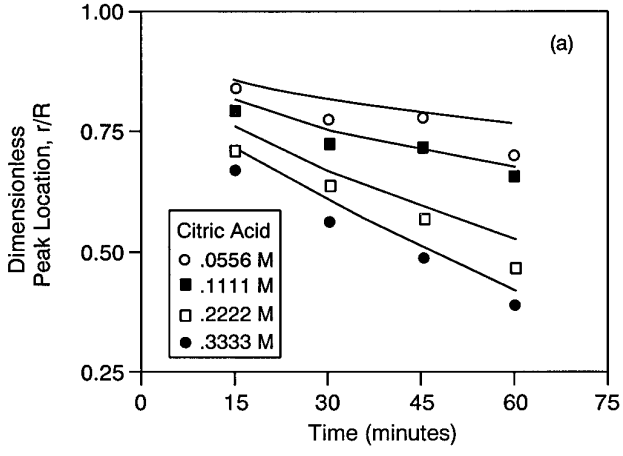

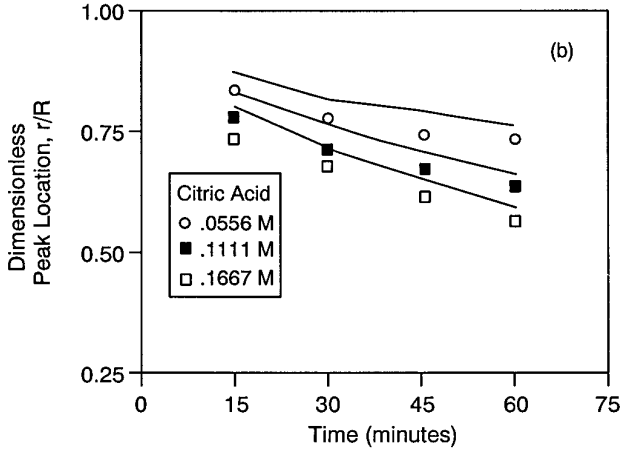

FIG. 8. Experimental platinum step locations and model predictions using 0.00589 *M* hexachloroplatinic acid and various citric acid concentrations: (a) sequential impregnation, (b) coimpregnation.

adsorption were decoupled. Specifically, diffusion coefficients were measured in the absence of adsorption, while adsorption constants were determined in the absence of diffusion resistances. In similar nonuniform catalyst preparation studies reported in the literature, adjustment of parameters was frequently employed in the diffusion–adsorption model. For example, Melo *et al.* (33) and Castro *et al.* (34) altered the single-component saturation coverages to fit the diffusion–adsorption model to the experimental data. Also, Chu *et al.* (15) required the use of larger effective diffusivity of hydrogen ions than typical values to fit distribution profiles of nickel in γ-Al_2O_3. However, their diffusion–adsorption model which took into account the surface chemistry by employing a triple-layer electrostatic model, showed excellent agreement on a qualitative level and in many cases also on a quantitative level with experimental distributions.

From the comparison of model predictions with experimental platinum profiles (Figs. 6–7), it may be seen that those determined by the model are wider. This may be due to the measurement procedure which uses optical microscopy. Schwarz and Heise (16) measured platinum profiles in γ-Al_2O_3 pellets using a scanning microdensitometer and found Pt distributions which resembled more the theoretical curves; i.e., the platinum was deposited not as a sharp band but more as a normal distribution with a tail toward the external surface of the pellet.

APPENDIX: NOTATION

c	liquid-phase concentration
D_e	effective diffusivity
D_m	molecular diffusivity
G	mass of support
K	k^+/k^-, equilibrium adsorption constant

K_1^{sol} k_1^{sol}/k^-, equilibrium adsorption constant due to solution effects
K_2^{st} equilibrium adsorption constant due to steric hinderances
k^+ adsorption rate constant
k^- desorption rate constant
k_1^{sol} desorption rate constant due to solution effects
L pellet length
M_p number of spherical pellets
n surface concentration
n_s surface saturation coverage
n_{ms} multicomponent surface saturation coverage
N_p number of cylindrical pellets
r radial distance
R pellet radius
t time
t_e impregnation time for equilibrium adsorption experiments
V volume of bulk solution
x axial distance

Subscripts

b bulk fluid
e equilibrium
i component i
j component j ($j \neq i$)
m multicomponent
0 for $t = 0$ s
p pore
1 hexachloroplatinic acid
2 citric acid
∞ for $t = \infty$ s

Superscripts

* at the end of the first impregnation in the sequential impregnation technique

Greek Letters

ε pellet porosity
λ stoichiometric factor
ρ_s density of the pellet
τ tortuosity factor

ACKNOWLEDGMENT

This work was supported by the National Science Foundation.

REFERENCES

1. Morbidelli, M., Servida, A., and Varma, A., *Ind. Eng. Chem. Fundam.* **21,** 278 (1982).
2. Morbidelli, M., Servida, A., Carra, S., and Varma, A., *Ind. Eng. Chem. Fundam.* **24,** 116 (1985).
3. Wu, H., Brunovska, A., Morbidelli, M., and Varma, A., *Chem. Eng. Sci.* **45,** 1855 (1990); see also **46,** 3328 (1991).
4. Baratti, R., Wu, H., Morbidelli, M., and Varma, A., *Chem. Eng. Sci.* **48,** 1869 (1993).
5. Gavriilidis, A., Varma, A., and Morbidelli, M., *Catal. Rev. -Sci. Eng.* **35,** 399 (1993).
6. Maatman, R. W., *Ind. Eng. Chem.* **51,** 913 (1959).
7. Michalko, E., U.S. Patent 3,259,589 (1966).
8. Becker, E. R., and Nuttall, T. A., *in* "Preparation of Catalysts II" (B. Delmon, P. Grange, P. A. Jacobs, and G. Poncelet, Eds.), p. 159. Elsevier, Amsterdam, 1979.
9. Shyr, Y.-S., and Ernst, W. R., *J. Catal.* **63,** 425 (1980).
10. Lee, S.-Y., and Aris, R., *Catal. Rev. -Sci. Eng.* **27,** 207 (1985).
11. Kulkarni, S. S., Mauze, G. R., and Schwarz, J. A., *J. Catal.* **69,** 445 (1981).
12. Hegedus, L. L., Chou, T. S., Summers, J. C., and Potter, N. M., *in* "Preparation of Catalysts II" (B. Delmon, P. Grange, P. A. Jacobs, and G. Poncelet, Eds.), p. 171. Elsevier, Amsterdam, 1979.
13. Scelza, O. A., Castro, A. A., Ardiles, D. R., and Parera, J. M., *Ind. Eng. Chem. Fundam.* **25,** 84 (1986).
14. Ruckenstein, E., and Karpe, P., *Langmuir* **5,** 1393 (1989).
15. Chu, P., Petersen, E. E., and Radke, C. J., *J. Catal.* **117,** 52 (1989).
16. Schwarz, J. A., and Heise, M. S., *J. Colloid Interface Sci.* **135,** 461 (1990).
17. Lemaitre, L. J., Menon, P. G., and Delannay, F., *in* "Characterization of Heterogeneous Catalysts" (F. Delannay, Ed.), p. 299. Dekker, New York, 1984.
18. Gavriilidis, A., Sinno, B., and Varma, A., *J. Catal.* **139,** 41 (1993).
19. Price, D. M., and Varma, A., *AIChE Symp. Ser.* **266,** 88 (1988).
20. Engels, S., Lausch, H., and Schwokowski, R., *Chem. Technik* (*Leipzig*) **39,** 387 (1987).
21. Jianguo, W., Jiayu, Z., and Li, P., *in* "Preparation of Catalysts III" (G. Poncelet, P. Grange, and P. A. Jacobs, Eds.), p. 57. Elsevier, Amsterdam, 1983.
22. Jiratova, K., *Appl. Catal.* **1,** 165 (1981).
23. Mang, Th., Breitscheidel, B., Polanek, P., and Knoezinger, H., *Appl. Catal. A* **106,** 239 (1993).
24. Subramanian, S., Noh, J. S., and Schwarz, J. A., *J. Catal.* **114,** 433 (1988).
25. Finlayson, B. A., "Nonlinear Analysis in Chemical Engineering." McGraw–Hill, New York, 1980.
26. "CRC Handbook of Chemistry and Physics," 67th ed. CRC Press, Boca Raton, FL, 1987.
27. Satterfield, C. N., "Heterogeneous Catalysis in Industrial Practice," 2nd ed., McGraw–Hill, New York, 1991.
28. Santacesaria, E., Galli, C., and Carra, S., *React. Kinet. Catal. Lett.* **6,** 301 (1977).
29. Foger, K., *in* "Catalysis Science and Technology, Vol. 6" (J. R. Anderson and M. Boudart, Eds.), p. 227. Springer-Verlag, Berlin, 1984.
30. Wilson, G. R., and Hall, W. K., *J. Catal.* **17,** 190 (1970).
31. Wanke, S. E., and Flynn, P. C., *Catal. Rev. -Sci. Eng.,* **12,** 93 (1975).
32. Kunimori, K., Nakajima, I., and Uchijima, T., *Chem. Lett.,* 1165 (1982).
33. Melo, F., Cervello, J., and Hermana, E., *Chem. Eng. Sci.* **35,** 2175 (1980).
34. Castro, A. A., Scelza, O. A., Benvenuto, E. R., Baronetti, G. T., De Miguel, S. R., and Parera, J. M., *in* "Preparation of Catalysts III" (G. Poncelet, P. Grange, and P. A. Jacobs, Eds.), p. 47. Elsevier, Amsterdam, 1983.
35. Santacesaria, E., Carra, S., and Adami, I., *Ind. Eng. Chem. Prod. Res. Dev.* **16,** 41 (1977).
36. Heise, M. S., and Schwarz, J. A., *J. Colloid Interface Sci.* **123,** 51 (1988).
37. Subramanian, S., and Schwarz, J. A., *Langmuir* **7,** 1436 (1991).